Biomimetic Nanochannels Based Biosensor for Ultrasensitive and Label-Free Detection of Nucleic Acids

Zhongyue Sun, Tangbin Liao, Yulin Zhang, Jing Shu, Hong Zhang, Guo-Jun Zhang

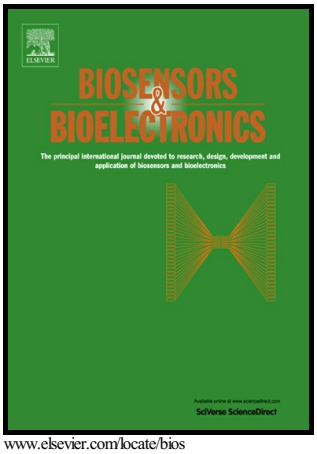

www.elsevier.com/locate/bios

PII: S0956-5663(16)30591-7
DOI: http://dx.doi.org/10.1016/j.bios.2016.06.059
Reference: BIOS8851

To appear in: *Biosensors and Bioelectronic*

Received date: 22 April 2016
Revised date: 7 June 2016
Accepted date: 19 June 2016

Cite this article as: Zhongyue Sun, Tangbin Liao, Yulin Zhang, Jing Shu, Hong Zhang and Guo-Jun Zhang, Biomimetic Nanochannels Based Biosensor for Ultrasensitive and Label-Free Detection of Nucleic Acids, *Biosensors and Bioelectronic,* http://dx.doi.org/10.1016/j.bios.2016.06.059

Biomimetic Nanochannels Based Biosensor for Ultrasensitive and Label-Free Detection of Nucleic Acids

Zhongyue Sun[a1], Tangbin Liao[a1], Yulin Zhang[a], Jing Shu[b], Hong Zhang[c*], Guo-Jun Zhang[a*]

[a]School of Laboratory Medicine, Hubei University of Chinese Medicine, 1 Huangjia Lake West Road, Wuhan 430065, China

[b]School of Nuring, Hubei University of Chinese Medicine, 1 Huangjia Lake West Road, Wuhan 430065, China

[c]Teaching and Research Office of Forensic Medicine, Hubei University of Chinese Medicine, 1 Huangjia Lake West Road, Wuhan 430065, China

zhanggj@hbtcm.edu.cn

redguo@hotmail.com

[*]Corresponding author. Tel.: +86-27-68890259, fax.: +86-27-68890259

[1] These authors contributed equally to this work.

Abstract

A very simple sensing device based on biomimetic nanochannels has been developed for label-free, ultrasensitive and highly sequence-specific detection of DNA. Probe DNA was modified on the inner wall of the nanochannel surface by layer-by-layer (LBL) assembly. After probe DNA immobilization, DNA detection was realized by monitoring the rectified ion current when hybridization occurred. Due to three dimensional (3D) nanoscale environment of the nanochannel, this special geometry dramatically increased the surface area of the nanochannel for immobilization of probe molecules on the inner-surface and enlarged contact area between probes and target-molecules. Thus, the unique sensor reached a reliable detection limit of 10 fM for target DNA. In addition, this DNA sensor could discriminate complementary DNA (c-DNA) from non-complementary DNA (nc-DNA), two-base mismatched DNA (2bm-DNA) and one-base mismatched DNA (1bm-DNA) with high specificity. Moreover, the nanochannel-based biosensor was also able to detect target DNA even in an interfering environment and serum samples. This approach will provide a novel biosensing platform for detection and discrimination of disease-related molecular targets and unknown sequence DNA.

Keywords: Nanochannels; Biosensor; Label-Free Detection; DNA; Hybridization

1. Introduction

Biological ion channels are functional protein complexes and embedded in cell membranes. Many ion channels are selective for a given ion or a molecule across the cell boundaries, so they play a crucial role in cellular metabolic processes and also become a model system to construct biosensors (Hiller and Sunderland, 2001; Kumar and Gilula, 1996). Nevertheless, this performance of ion channels only exists on live cell membrane, which severely handicaps its development and practical application. To work around those problems, a number of artificial biomimetic nanochannels, inspired by biological ion channels have been designed (Hou, 2013; Hou et al., 2012; Daiguji, 2010; Howorka and Siwy, 2009). Because of their robust mechanical and chemical properties, some biosensors and other nanodevices have been reported and triggered enormous research interests (Inglis et al., 2011; Wei et al., 2012; Jiang et al., 2012; Haywood et al., 2015). Comparing with other biosensors, the nanochannel-based biosensors have special three dimensional (3D) nanoscale environment (Guo et al., 2015; Nie et al., 2015; Zhang et al., 2015). For instance, this special geometry dramatically increases the surface area of nanochannel for immobilization of probe molecules on the inner-surface and enlarges contact area between probes and target-molecules (Kim et al., 2015). Such a great property is very useful for building a

highly sensitive and specific biosensor. Therefore, it is desirable to develop the nanochannel-based biosensor for high sensitive and specific detection of biomolecules (Sun et al., 2014; Liu et al., 2015; Sun et al., 2015; Gao et al., 2015; Wang et al., 2015; Sun et al., 2012; Ali et al., 2015; Xu et al., 2015; Ali et al., 2015).

Sequence-specific nucleic acids detection and analysis have become a hot topic and caught much attention due to their widespread applications in the fields of molecular biology, disease diagnosis, pathogen detection, forensic analysis, food industry and so on (Bowtell, 1999; Lam et al., 2013; Janasek et al., 2006; Drummond et al., 2003; Hay Burgess et al., 2006). Nowadays, various biosensors have been used for nucleic acids detection such as electrochemical sensors (Pollet et al., 2009; Yang et al., 2014; Daniels et al., 2007; Pourmand and Fan, 2008; Berggren et al., 1998), field-effect transistor (FET) biosensor (Cai et al., 2014; Zheng et al., 2015; Cai et al., 2015; Zhang et al., 2010), optical systems (Huang et al., 2011; Akhavan et al., 2012; Panke et al., 2007; Aoki and Tao, 2007; Feng et al., 2008). In particular, most of them usually introduce one dimensional (1D) or two dimensional (2D) nanomaterials to improve sensitivity, and realize label-free detection, because of nanostructure's unique properties. Nevertheless, development of nucleic acids biosensor with high sequence specificity and sensitivity is still a challenge. It is expected that 3D nanoscale environment benefits immobilization of more probe molecule on the small surface of

the nanostructures and transportation of more target molecule to the sensing interface, thus improving the detection sensitivity and specificity.

Recently, the highly specific and sensitive nanochannels based biosensors have been developed as efficient sensing platforms in detecting nucleic acids (Xia et al., 2013; Ali et al., 2014; Farimani et al., 2010). The principle of the nanochannel-based DNA biosensors is that the immobilized probe specifically hybridizes with single-stranded target nucleic acids on the channel surface. The hybridization event changes the surface charge density and/or effective diameter of the nanochannel, and triggers the membrane current change, which can be recorded by instrument. For instance, Xia et al. (Xia et al., 2013) developed a novel nanochannel-based method for detecting oligonucleotides through forming complex supersandwich structures capable of blocking the nanochannel. And this system could also detect DNA in complex matrices and serum sample. But this sensing strategy had to introduce multiple probes to construct complex DNA nanostructure inside the nanochannel. Ali and co-workers (Ali et al., 2014) reported a simple, highly selective and label-free sensing system, in which peptide nucleic acid (PNA)-modified nanochannel was proposed for the sequence-specific detection of DNA. Very unfortunately, this method does not further investigate the method's sensitivity and involve the real sample detection. It is still a challenge to develop a simple, cost-effective and label-free nanochannel biosensor for

DNA sensing with high sensitivity and specificity in both buffer and complex real sample.

Herein, we demonstrate a very simple and facile strategy to fabricate a novel nanochannel sensing platform for label-free detection of DNA with high sequence-specificity and sensitivity. Moreover, the nanochannel-based biosensor is also able to detect target DNA even in an interfering environment and serum samples. In the present work, the probe DNA is modified on the channel surface by layer-by-layer (LBL) assembly (Ali et al., 2010), which is a very straightforward and effective strategy for functionalization of the nanochannel surface. This method avoids the requirements for complex chemical steps in modification process. In order to improve sequence-specificity and restrain interference, the DNA-modified membrane is incubated with bovine serum albumin (BSA) to prevent possible nonspecific binding events by blocking the active sits on the channel surface. The high sequence specificity of this system is subsequently demonstrated by using the complementary, one-base mismatched, and noncomplementary DNA sequences. Most significantly, even in complex matrices and real sample, this biosensor also shows highly specific response and negligible interference.

2. EXPERIMEATAL SECTION

2.1. Materials and DNA Sequences

Poly(ethylene terephthalate) (PET, 12 μm thick) membranes were irradiated with Ar ion beam of energy 18 MeV/nucleon (Tsinghua University, Beijing, China). The track density is about $4\times10^5/cm^2$. All DNAs were 16-mer in length and diluted with 0.1 M KCl prepared in PBS (pH 7.0). The sequence of the DNA probe is 5'-CACAAAACGGGGGCGG-3'. The sequences of the DNAs employed for hybridization are 5'-CCGCCCCCGTTTTGTG-3' (complementary, c-DNA), 5'-CCGCACCCATTTTGTG-3' (two-base mismatched, 2bm-DNA), 5'-CCGCCCCCATTTTGTG-3' (one-base mismatched, 1bm-DNA), 5'-AATAAAAATGGGGTGT-3' (non-complementary, nc-DNA). BSA and polyethyleneimine (PEI) were purchased from Sigma-Aldrich. Sodium hydroxide (NaOH), hydrochloric acid (HCl), formic acid (HCOOH), potassium chloride (KCl), sodium dihydrogen phosphate (NaH_2PO_4), and sodium hydrogen phosphate (Na_2HPO_4) were purchased from Sinopharm Chemical Reagent Shanghai Co. Ltd. (SCRC, China). All solutions were prepared in MilliQ water (18.2 MΩ).

2.2. Fabrication of conical nanochannels

The conical nanochannels were prepared by chemical etching of 12 μm thick PET membrane (Wharton et al., 2007). Before etching process, each side of the PET membranes was exposed in UV light (365 nm) for 1 h. In order to obtain the conical nanochannel, etching was performed only from one side. The other side of the cell

contained a solution that was able to neutralize the etchant as soon as the pore was opened, thus slowing down the further etching process. The PET membrane was embedded between the two chambers of a conductivity cell at 30 °C, in which one chamber was filled with etching solution (9 M NaOH), and the other chamber was filled with stopping solution (1 M KCl + 1 M HCOOH). Then a voltage of 1 V was applied across the membrane. The etching process was stopped at a desired current value corresponding to a certain tip diameter. The membrane was immerged in distilled water to remove residual salts. The large opening of the conical nanochannel was called base (D) and the small opening was called tip (d_{tip}). Field emission-scanning electron microscopy (FE-SEM) was used to characterize the nanochannel size of both sides. As seen in Figure S1, the base diameter was found to be about 1.2 μm and the tip diameter was about 45 nm.

2.3. Modification of Nanochannels

After the chemical etching process, the track-etched nanochannel film was immersed in an aqueous solution of the PEI (1 mg/mL, pH 7.0), and allowed to self-assemble overnight. After adsorption of PEI, the membrane was washed with distilled water several times. A solution of probe DNA (10 μM, pH 7.0) was then added on the both sides of PEI modified channel and allowed for incubation for 2 h. The membrane was washed with distilled water to remove unreacted probe DNA and then incubated

with 10 mg/ml BSA solution (pH 9.0) for 1 h to prevent possible nonspecific binding events and then washed by distilled water. To determine the success of the assembly process, the current-voltage (I-V) curves were measured by using 0.1 M KCl (pH 7.0) as electrolyte.

2.4. DNA-DNA hybridization

The probe DNA-modified nanochannel membrane was exposed to nc-DNA solutions and incubated for 1 h at 37 °C. After hybridization, the channel was washed with 0.1 M KCl (pH 7.0) solution and distilled water to remove the unhybridized DNA. After washing, the ion flux was measured using 0.1 M KCl (pH 7.0) as an electrolyte. The same procedure was repeated, when 2bm-DNA, 1bm-DNA and c-DNA were hybridized with probe DNA on the channel surface, respectively.

2.5. Ion currents measurement

Ion currents were measured by a Keithley 6487 picoammeter (Keithley Instruments, Cleveland, OH). Ag/AgCl electrodes were used to apply a transmembrane potential across the film. PET film was mounted between the two halves of the conductance cell. Both halves of the cell were filled with electrolyte solution 0.1 M KCl (pH 7.0). Then the data record was carried out with a scanning triangle voltage signal from -1 V to +1 V with a 40 s period in 0.1 M KCl (pH 7.0). Each test was repeated 5 times to obtain the average current value at different voltage.

2.6. Characterizations

The nanochannel diameter was determined by FE-SEM (Zeiss SIGMA, Germany). X-ray photoelectron spectroscopy (XPS) spectra of the nanochannels were obtained by an ESCALAB 250Xi XPS (Thermo Fisher, America) and the source gun types were Al and Ka. Laser scanning confocal microscopy (LSCM) of the inner membrane surface were obtained by using a Zeiss confocal laser scanning unit mounted on a LSM710 fixed-stage upright microscopy.

3. RESULTS AND DISCUSSION

3.1.Mechanism

The working mechanism of the nanochannel-based biosensor for ultrasensitive and label-free detection of DNA is depicted in Fig. 1. At first, the conical nanochannels are prepared by chemical etching of 12 μm thick PET membrane. After the chemical etching process, ionized carboxyl groups ($-COO^-$) are exposed on the unmodified conical-shaped PET nanochannel surface, resulting in a negatively charged surface at pH 7.0. Secondly, positively charged PEI is self-assembled on the channel surface by electrostatic interaction, triggering a change in the polarity of the nanochannel from negative to positive. After that, negatively charged probe DNA is further assembled on the positively charged channel surface and negatively charged BSA is used for blocking, making the positive charge on the surface less. When target

DNA is hybridized with probe DNA, the surface charge and charge density dramatically change due to the contribution of negatively charged phosphate backbone of the DNA nucleotide. The hybridization between probe and target is monitored by recording the current-voltage (I-V) curves.

3.2.Modification of Nanochannels

In this experiment, the I-V curve of the bare nanochannel acted as the control. The unmodified conical-shaped PET nanochannel surface was negatively charged. Thus it slightly rectified the ionic current (Fig. 2A). After self-assembling positively charged PEI at pH 7.0 on the channel surface, a change in the charge of the nanochannel from negative to positive was obtained. The immediate inversion of the rectifying characteristics indicates that the successful assembly of PEI on the nanochannel surface is carried out. Afterwards, probe DNA was easily absorbed on PEI layer by static interaction, and BSA was employed to block the unmodified sites on the surface. Upon introduction of DNA and BSA, the charge on the inner channel surface significantly decreased, leading to a significant decrease in the ion current and the curve was observed to be almost a straight line (Fig. 2A). This means that the negatively charged phosphate backbone of DNA and the negatively charged BSA molecule diminish the positive channel surface charge, leading to a decrease in the rectified ionic current. $R_{-/+}$ reflects the extent of rectification (permselectivity) of the

conical nanochannels. The value of $R_{-/+}$ (defined as the absolute value of the current at -1 V divided by the current at +1 V) is sensibly correlated with the surface charge. Consequently, a slight increase/decrease in surface charge can trigger a marked increase/decrease in rectification ratio of the nanochannel. Fig. 2B. shows the rectification ratio $R_{-/+}$ of the conical nanochannel. Before modification, the channel surface was negatively charge, thus it slightly rectified and the $R_{-/+}$ was about 2.95. After PEI was assembled on the inner wall, the charge of the nanochannel changed from negative to positive. The rectifying characteristics inversed and $R_{-/+}$ changed to 0.20. When probe DNA was modified, the surface charge remarkably decreased, leading to a significant decrease in the ion current and the curve was shown to be almost a straight line. So the value of $R_{-/+}$ was close to 1, resulting in the less rectifying characteristics. The results indicate that the continuous assembly process is successfully realized.

To further verify the success of LBL assembly process, XPS was used to evaluate the chemical composition of PET film (Fig. S2). Fig. S2A shows wide energy XPS spectra of each functionalized process. In this experiment, the XPS characterizations were conducted on the unmodified nanochannel membrane as the control (black line), PEI modified film (green line), and probe DNA self-assembly membrane (wine red line), respectively. On the unmodified PET film surface, only C 1s and O 1s peaks

were clearly observed. Narrow energy spectra comparing N1s peaks between the bare PET film and the PEI-modified one were shown in the Fig. S2B. It was clearly seen that after PEI was introduced to the channel surface (green line), a N 1s (399 eV) peak appeared, meaning that PEI was modified on the surface as anticipated. The probe self-assembly on the channel surface was also verified by narrow energy spectra of the PEI-modified film and the probe DNA- assembled one (Fig. S2C). The presence of P 2p (133 eV) peaks on the probe-modified film (wine red line) further indicated the probe DNA was immobilized on the surface of the PET nanochannel. All the above data verify the success of LBL assembly process on the surface of the PET nanochannel.

3.3.Stability of modified nanochannel

We also investigated the stability of the probe DNA-modified nanochannel in terms of the voltage and current signals with respect to time in 0.1 M KCl, pH 7.0, by applying a scanning voltage varying from −1 V to +1 V for 520 s. As shown in Fig. S3, the amplitude and shape of the current curve (black trace) showed negligible change. The data show that the functionalized nanochannel sensor is stable and can be used for DNA detection.

3.4.Verification of DNA-DNA hybridization by fluorescent imaging

The hybridization event occurring on the inner surface of nanochannel was verified by LSCM. As shown in Fig. 3, Cy3 fluorophore labeled target DNA (Cy3-DNA) was used to hybridize with the immobilized probe DNA. When the probe modified nanochannel was incubated with 0.1 M KCl, pH 7.0, negligible fluorescent signal was seen. However, the strong fluorescent signal appeared after hybridization, indicating that the Cy3-DNA has successfully been hybridized with the probe DNA on the nanochannel surface. In addition, the fluorescent signal showed the membrane thickness was ca. 12.3± 0.5 μ m, which agrees with its actual thickness (Fig. 3B). The data demonstrate that c-DNA has been hybridized with probe DNA on the nanochannels surface.

3.5.Optimization of DNA biosensor conditions

PH is always related to the protonation of PEI and phosphate backbone of DNA and exerts significant impact on the surface charge and charge density. Therefore, the effect of varying pH (5.0, 6.0, 7.0, 8.0, 9.0) on the PEI-modified nanochannel sensor was studied by relative $R_{-/+}$ change ratios (ratios defined by $(R–R_0)/ R_0$, where R_0 is the initial rectification ratio, R is the rectification ratio after treating with DNA strands, respectively.) in a solution containing 1 nM c-DNA for 1 h at 37 °C, respectively (Fig. S4A). The maximum $R_{-/+}$ change ratios for c-DNA were found to be at pH 7.0. That could be ascribed to enhanced protonation of phosphate groups of

DNA at acidic condition. While electrostatic interaction between probe DNA and PEI was reduced at basic condition because the positive charge of PEI decreased. Therefore, pH 7.0 was chosen for the determination of DNA in this work.

The hybridization time and temperature of the nanochannel sensor were also investigated, respectively. As shown in Fig. S4B, when 1 nM c-DNA was interacted with the sensor at pH 7.0, and the hybridization temperature was fixed at 37 °C, the $R_{-/+}$ change ratios obviously increased with the increasing hybridization time from 30 to 100 min. The hybridization tended to be stable after 60 min, indicating that the hybridization reaction was nearly completed in 60 min. The effect of the varying hybridization temperature (25-55°C) on $R_{-/+}$ change ratios of c-DNA was also investigated. As shown in Fig. S4C, the maximal $R_{-/+}$ change ratios occurred between 37 and 45 °C, but the difference of $R_{-/+}$ change ratios at 37 and 45 °C seemed to be very slight. In this system, the hybridization temperature was chosen as 37 °C by considering the normal body temperature.

3.6.Specificity

The specificity of the nanochannel for label-free recognition of DNA was investigated by transmembrane ion current in 0.1 M KCl, pH 7.0 (Fig. 4A). The functionalized nanochannel membrane was immersed in 1 nM nc-DNA, 2bm-DNA, 1bm-DNA, and fully complementary (c-DNA) oligomers solution for 1 h at 37 °C,

respectively. Then, the film was washed with 0.1 M KCl, pH 7.0 to remove physically adsorbed DNA molecules. The hybridization on the channel surface was monitored by transmembrane current. Fig. 4A shows the ion current of the probe DNA modified nanochannel incubated with 0.1 M KCl, pH 7.0, 1 nM nc-DNA, 2bm-DNA, 1bm-DNA and c-DNA, respectively. In this experiment, 0.1 M KCl, pH 7.0 acted as the control (black line). Upon exposure of the modified channels to nc-DNA oligomer solution, only slight change in I-V characteristics was observed. The small current change might come from some nonspecific adsorption. When this same experiment was conducted in the presence of c-DNA, the transmembrane ionic current increased very significantly. Fig. 4B shows the relative $R_{-/+}$ change ratios of the modified nanochannel in the presence of 1 nM concentration of the above DNA strands. For 1bm-DNA, $R_{-/+}$ change ratio was larger than that of nc-DNA, but still much smaller than that of c-DNA. Although 1bm-DNA could hybridize with probe and form a duplex on the channel surface, this structure was unstable and could be unzipped during the washing. When interacted with two-base mismatched sequence, the duplex between 2bm-DNA and probe was much less stable, $R_{-/+}$ change ratio of 2bm-DNA was smaller than that of 1bm-DNA. It is obvious that the $R_{-/+}$ change ratios for c-DNA was much larger than those of nc-DNA, 2bm-DNA and 1bm-DNA. The data indicate

that the nanochannels as the nucleic acids sensor can distinguish c-DNA from nc-DNA, and bm-DNA, exhibiting a remarkable specificity.

3.7.Sensitivity

The sensitivity of the nanochannel-based biosensor was investigated by adding various concentrations of c-DNAs (from 1 fM to 1 nM) to hybridize with the probe-DNA functionalized nanochannel. And the results were shown in Fig. 5. Rectified ion current (measured at -1 V) and $R_{-/+}$ change ratios generally increased as the concentrations of the c-DNAs were increased from 1 fM to 1 nM. In a certain concentration range, the modified nanochannel displayed a response to c-DNA. The detection limit was determined according to the method reported in literature (Xia et al., 2013). When nc-DNA oligomer was interacted with the probe DNA-modified nanochannel, the $R_{-/+}$ change ratio of nc-DNA was found to be about 0.48. It is very clear that the $R_{-/+}$ change ratio is probably caused by non-specific adsorption. If the ratio is above 0.48, an effective and reliable detection occurs and the ratio (0.5) is defined as a threshold. In this experiment, when 1 fM c-DNA was interacted with the probe DNA-modified nanochannel, the $R_{-/+}$ change ratio was about 0.46 (< 0.5). However, upon addition of 10 fM c-DNA to incubate with the functioned channel sensor, the $R_{-/+}$ change ratio was about 0.97 (> 0.5). According to the above discussion, the detection limit was determined to be 10 fM (Fig. 5B).

Radecki et al. (Radecki et al., 2015) developed an electrochemical based ion barrier switch-off system for DNA detection with a detection limit of 1.99 pM. He and Ma (He and Ma, 2014) used quantum dot (QD) doping-induced photoluminescence for DNA detection with detection sensitivity of 10 pM. Song et al. (Song et al., 2014) reported a label-free and non-enzymatic amplification fluorescent method based on hybridization chain reaction (HCR) amplification technique and fluorescence copper nanoparticles (CuNPs) as indicators for DNA detection. Target DNA could trigger HCR process and formed dsDNA polymers on the beads. Then, CuNPs were synthesized on dsDNA polymers resulting in significantly amplified fluorescence signal. This method was sensitive and specific to target DNA with a detection limit of 0.4 nM. A label-free colorimetric method for highly sensitive detection of DNA by coupling target-catalyzed hairpin assembly and ExoIII-assisted signal amplification was developed by Wu et al. (Wu et al., 2015). This method could discriminate mismatched DNA from target DNA and exhibits a high sensitivity with a low detection limit of 81 fM. Ju et al. (Ju et al., 2013) constructed probe DNA-Ag nanoparticle-graphene oxide modified interface for DNA detection (limit of detection LOD 1 pM) through surface-enhanced raman spectroscopy (SERS) method. Our group has recently proposed a reduced graphene oxide (R-GO) field-effect transistor (FET) biosensor for label-free detection of DNA with ultra sensitivity and high

specificity (Zhang et al., 2014). This system applied R-GO nanomaterial to amplify detection signal and introduced peptide nucleic acid (PNA) instead of DNA as the capture probe to enhance the specificity and sensitivity. The detection limit as low as 100 fM was achieved.

The various methods for DNA sensing based on DNA-DNA hybridization are illustrated in Table S1. Compared with other label-free DNA detection methods, the nanochannel-based DNA sensor has special 3D nanoscale environment. Not only is the sensor unnecessary to introduce signal amplification strategy, but also it could reach a reliable detection limit of 10 fM for target DNA. The sensitivity of the developed method is about 1 order of magnitude higher than those reported by FET and colorimetric, respectively, 3 orders of magnitude higher than that reported by photoluminescence, and 4 orders of magnitude higher than that reported by electrochemistry.

3.8.Interference and serum sample analysis

In order to further investigate the practical application of the nanochannel-based biosensor, we challenged DNA detection in interfering system and serum samples. In this experiment, 1 nM c-DNA was mixed with 100 nM nc-DNA solution, and the high concentration of nc-DNA acted as interfering substance. As shown in Fig. 6A, when the modified nanochannels was interacted with the interfering substance without

target DNA, the $R_{-/+}$ change ratio was below the threshold of 0.5. So it is clear that this phenomenon takes place probably due to non-specific adsorption. A significant signal changed, after the same nanochannel was incubated with the solution containing 1 nM c-DNA and 100 nM interfering substances. The results indicate the biosensor presents an ability of anti-interference when challenged in interfering system.

In 5% fetal bovine serum sample containing 1pM and 1nM c-DNA, the sensor still maintained high detection ability to target DNA. Fig. 6B shows the $R_{-/+}$ change ratios of the nanochannel incubated with 1 pM and 1 nM target DNA in electrolyte and 5 % fetal bovine serum sample, respectively. The $R_{-/+}$ change ratios of 1 pM and 1 nM target DNA in serum sample were smaller than those in electrolyte. This is due to the fact that serum is a very complex mixture, and the multicomponent could degrade the performance of DNA sensing. Hence, the hybridization efficiency of probe DNA with target DNA in serum might decrease compared with that in electrolyte. Nevertheless, the biosensor still works well in both interfering system and serum samples, showing that it has the potential of being applied in the practical applications.

4. CONCLUSIONS

In summary, we have presented a very simple and facile strategy to fabricate a novel nanochannel-based sensing platform for label-free detection of DNA in confined 3D nanospace with high sequence-specificity and sensitivity. And this biosensor also showed high response and robust anti-interference when challenged in interfering system and serum samples. The unique 3D geometry of nanochannels enlarged surface area for the functionalization of probe and thus improved the affinity between probe and target molecule. The probe-DNA functionalized nanochannel could discriminate c-DNA from nc-DNA, 2bm-DNA and 1bm-DNA strands with high selectivity by monitoring the rectified ion flux upon hybridization on the channel surface. Moreover, a reliable detection limit of 10 fM for target DNA was achieved. It is expected that this approach has universal applications in detecting other disease-related molecular targets.

Acknowledgements

This work was supported by the National Natural Science Foundation of China (Nos. 21405037, 21275040 and 21475034).

Supporting Information

Supplementary data associated with this article can be found in the online version at

References

Akhavan, O., Ghaderi, E., Rahighi, R., 2012. ACS Nano 6, 2904-2916.

Ali, M., Ahmed, I., Nasir, S., Ramirez, P., Niemeyer, C. M., Mafe, S., Ensinger, W., 2015. ACS Appl. Mater. Interfaces 7, 19541-19545.

Ali, M., Nasir, S., Ensinger, W, 2015. Chem. Commun. 51, 3454-3457.

Ali, M., Neumann, R., Ensinger, W., 2010. ACS Nano 4, 7267-7274.

Ali, M., Yameen, B., Cervera, J., Ramirez, P., Neumann, R., Ensinger, W., Knoll, W., Aoki, H., Tao, H., 2007. Analyst. 132, 784-791.

Azzaroni, O., 2010. J. Am. Chem. Soc. 132, 8338-8348.

Berggren, C., Bjarnason, B., Johansson, G., 1998. Biosens. Bioelectron. 13, 1061-1068.

Bowtell, D. D. 1999. Nat. Genet. 21, 25-32.

Cai, B., Huang, L., Zhang, H., Sun, Z., Zhang, Z., Zhang, G. J., 2015. Biosens. Bioelectron. 74, 329-334.

Cai, B., Wang, S., Huang, L., Ning, Y., Zhang, Z., Zhang, G. J., 2014. ACS Nano 8, 2632-2638.

Daiguji, H., 2010. Chem. Soc. Rev. 39, 901-911.

Daniels, J. S., Pourmand, N., 2007. Electroanalysis 19, 1239-1257.

Drummond, T. G., Hill, M. G., Barton, J. K., 2003. Nat. Biotechnol. 21, 1192-1199.

Fan, X., White, I. M., Shopova, S. I., Zhu, H., Suter, J. D., Sun, Y., 2008. Anal. Chim. Acta. 620, 8-26.

Farimani, A. B., Min, K., Aluru, N. R., 2014. ACS Nano 8, 7914-7922.

Feng, F., He, F., An, L., Wang, S., Li, Y., Zhu, D., 2008. Adv. Mater. 20, 2959-2964.

Gao, F. L., Lei, J. P., Ju, H. X., 2013. Anal. Chem. 85, 11788-11793.

Gao, L. J., Li, P., Zhang, Y. Q., Xiao, K., Ma, J., Xie, G. H., Hou, G. L., Zhang, Z., Wen, L. P., Jiang, L., 2015. Small 1, 543-547.

Guo, Wei., Hong, F., Liu N. N., Huang, J. Y., Wang, B., Duan, R. X., Lou, X. D., Xia, F., 2015. Adv. Mater. 12, 2090-2095.

Hay Burgess, D. C., Wasserman, J., Dahl, C. A., 2006. Nature 444, 1-2.

Haywood, D. G., Saha-Shah, A., Baker, L. A., Jacobson, S. C., 2015. Anal. Chem. 87, 172-187.

He, X. W., Ma, N., 2014. Anal. Chem. 86, 3676-368.

Hiller, B., Sunderland, M. A., 2001. Ion Channels of Excitable Membranes, third ed. Sinauer.

Hou, X., Zhang , H. C., Jiang, L., 2012. Angew. Chem. Int. Ed. 51, 5296-5307.

Hou, X. 2013. Bio-inspired Asymmetric Design and Building of Biomimetic Smart Single Nanochannels, Springer Theses, Springer Berlin.

Howorka, S., Siwy, Z. S., 2009, Chem. Soc. Rev. 38, 2360-2384.

Huang, J., Wu, Y., Chen, Y., Zhu, Z., Yang, X., Yang, C. J., Wang, K., Tan, W., 2011, Angew. Chem., Int. Ed. 50, 401-404.

Inglis, D. W., Goldys, E. M., Calander, N. P., 2011. Angew. Chem. Int. Ed. 50, 7546-7550.

Janasek, D., Franzke, J., Manz, A., 2006. Nature 442, 374-380.

Jiang, Y. N., Liu, N. N., Guo, W., Xia, F., Jiang, L., 2012. J. Am. Chem. Soc. 134, 15395-15401.

Kim, B. Y., Sohn I. Y., Lee, D., Han, G. S., Lee, W. I., Jung, H. S., Lee, N. E., 2015. Nanoscale 7, 9844-9851.

Kumar, N. M., Gilula, N. B., 1996. Cell 84, 381-388.

Kurzatkowska, K., Sirko, A., Zagorski-Ostoja, W., Dehaen, W., Radecka, H., Radecki, J., 2015. Anal. Chem. 87, 9702-9709.

Lam, B., Das, J., Holmes, R. D., Live, L., Sage, A., Sargent, E. H., Kelley, S. O. 2013. Nat. Commun. 4, 2001-2008.

Liu, N. N., Jiang, Y. N., Zhou, Y. H., Xia, F., Guo, W., Jiang, L., 2013. Angew. Chem. Int. Ed. 52, 2007-2011.

Liu, N. N., Yang, Z. K., Lou, X. D., Wei, B. M., Zhang, J. T., Gao, P. C., Hou, R. Z., Xia, F., 2015. Anal. Chem. 87, 4037-4041.

Nie, G. R., Sun, Y., Zhang, F., Song, M. M., Tian, D. M., Jiang, L., Li, H. B., 2015.

Chem. Sci. 6, 5859-5865.

Panke, O., Kirbs, A., Lisdat, F., 2007. Biosens. Bioelectron. 22, 2656 -2662.

Pollet, J., Delport, F., Janssen, K. P. F., Jans, K., Maes, G., Pfeiffer, H., Wevers, M., Lammertyn, J., 2009. Biosens. Bioelectron. 25, 864-869.

Song, C., Yang, X. H., Wang, K. M., Wang, Q., Huang, J., Liu, J. B., Liu, W., Liu, P., 2014. Anal. Chim. Acta 827, 74-79.

Sun, Z. Y., Han, C. P., Song, M. M., Wen, L., Tian, D. M., Li, H. B., Jiang, L., 2014. Adv. Mater. 26, 455-460.

Sun, Z. Y., Han, C. P., Wen, L., Tian, D. M., Li, H. B., Jiang, L., 2012. Chem. Commun. 48, 3282-3284.

Sun, Z. Y., Zhang, F., Zhang, X. Y., Tian, D. M., Li, H. B., Jiang, L., 2015. Chem. Commun. 51, 4823-4826.

Wang, H. M., Hou, S. N., Wang, Q. Q., Wang, Z. W., Fan, X., Zhai, J., 2015. J. Mater. Chem. B. 3, 1699-1705.

Wei, R. S., Gatterdam, V., Wieneke, R., Tampe, R., Rant, U., 2012. Nat. Nanotechnol. 7, 257-263.

Wharton, J. E., Jin, P., Sexton, L. T., Horne, L. P., Sherrill, S. A., Mino W. K., Martin, C. R., 2007. Small 3, 1424-1430.

Wu, H., Liu, Y. L., Wang, H. Y., Wu, J., Zhu, F. F., Zou, P., 2015. Biosens.

Bioelectron. 66, 277-282.

Xu, Y. L., Sui, X., Guan, S., Zhai, J., Gao, L. C., 2015. Adv. Mater. 27, 1851-1855.

Yang, F., Yang, X., Wang, Y., Qin, Y., Liu, X., Yan, X., Zou, K., Ning, Y., Zhang, G. J. 2014. Anal. Chem. 86, 11905-11912.

Zhang, G. J., Luo, Z. H. H., Huang, M. J., Tay, G. K. I., Lim, E. J. A., 2010. Biosens. Bioelectron. 25, 2447-2453.

Zhang, H. C., Tian, Y., Hou, J., Hou, X., Hou, G. L., Ou, R. W., Wang, H. T., Jiang, L., 2015. ACS Nano 9, 12264-12273.

Zheng, C., Huang, L., Zhang, H., Sun, Z. Y., Zhang, Z. Y., Zhang, G. J., 2015. ACS Appl. Mater. Interfaces 7, 16953-16959.

Fig. 1. Schematic illustration of the probe DNA functionalized nanochannel biosensor for DNA detection.

Fig. 2. A) Current-voltage (I-V) and B) rectifying characteristics of the LBL assembly process on the conical nanochannel. I-V curve of the bare nanochannel acted as the control. $R_{-/+}$ defined as the absolute value of the current at -1 V divided by the current at +1 V. The immediate inversion and tremendous decrease about I-V curve prove the success of the continuous assembly process.

Fig. 3. LSCM observation of the nanochannels before A) and after B) Cy3 fluorophore labeled target DNA hybridized with probe on the channel surface. Strong fluorescent signal from the cross-sectional view proves the successful assembly inside the nanochannels.

Fig. 4. A) I-V curves of the nanochannels after treated with 1 nM nc-DNA, 2bm-DNA, 1bm-DNA, and c-DNA for 1 h at 37 °C, respectively. In this experiment, 0.1 M KCl, pH 7.0 acted as the control (black line). B) $R_{-/+}$change ratios measured in 0.1 M KCl pH 7.0 of the modified nanochannel in the presence of 1 nM concentration of the above DNA strands.

Fig. 5. A) I-V curves of the nanochannel biosensor hybridized with c-DNA at a series of concentrations (1 fM-1 nM), and B) The corresponding $R_{-/+}$ change ratios versus various concentrations. In a certain concentration range, the modified nanochannel sensor displayed a response to c-DNA.

Fig. 6. $R_{-/+}$ change ratios measured A) without or with the addition of 1 nM target DNA in 100 nM interfering sequences (nc-DNA prepared in 0.1 M KCl, pH 7.0) respectively. B) $R_{-/+}$change ratios measured in both electrolyte and 5% serum sample containing 1 pM and 1 nM c-DNA.

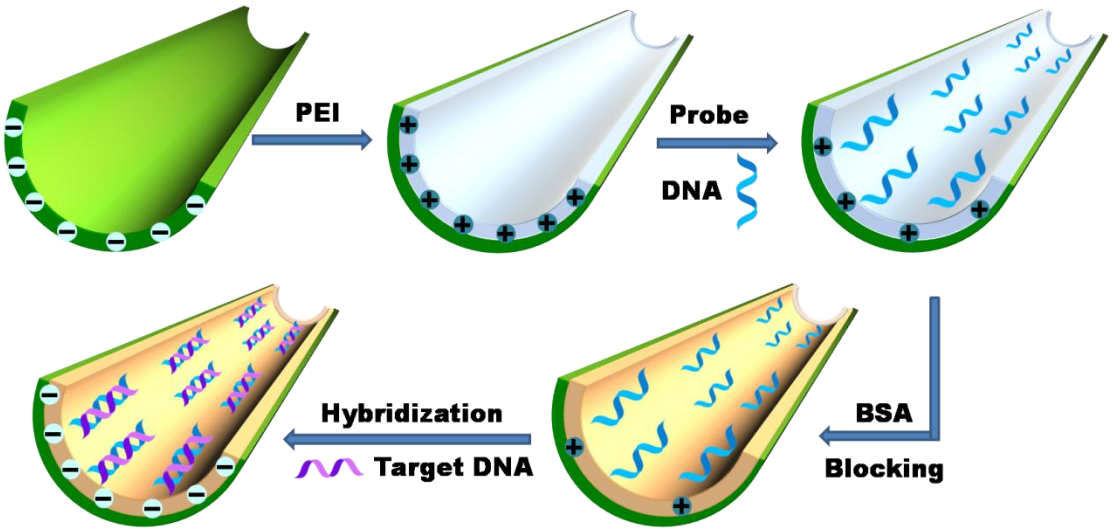

Fig.1

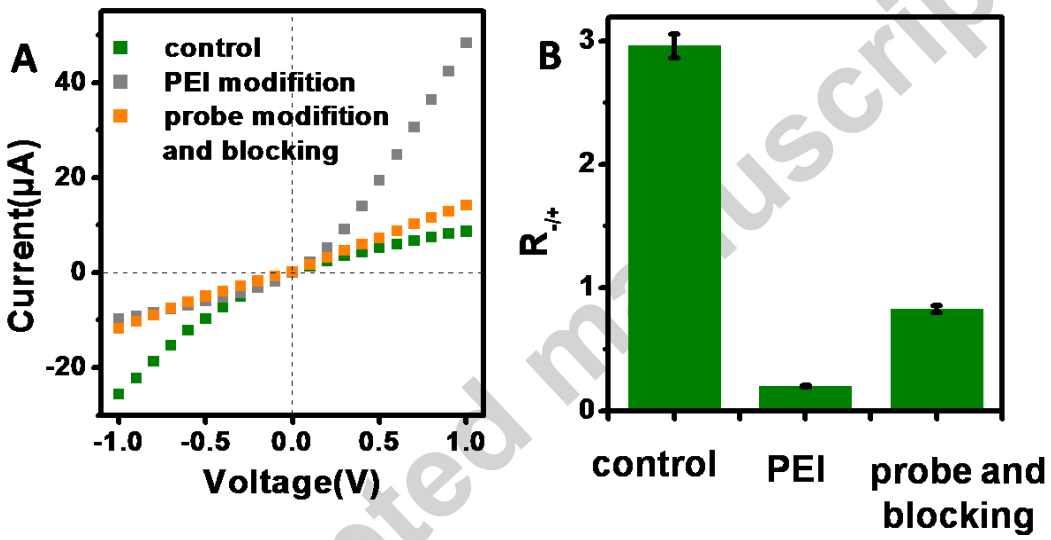

Fig. 2

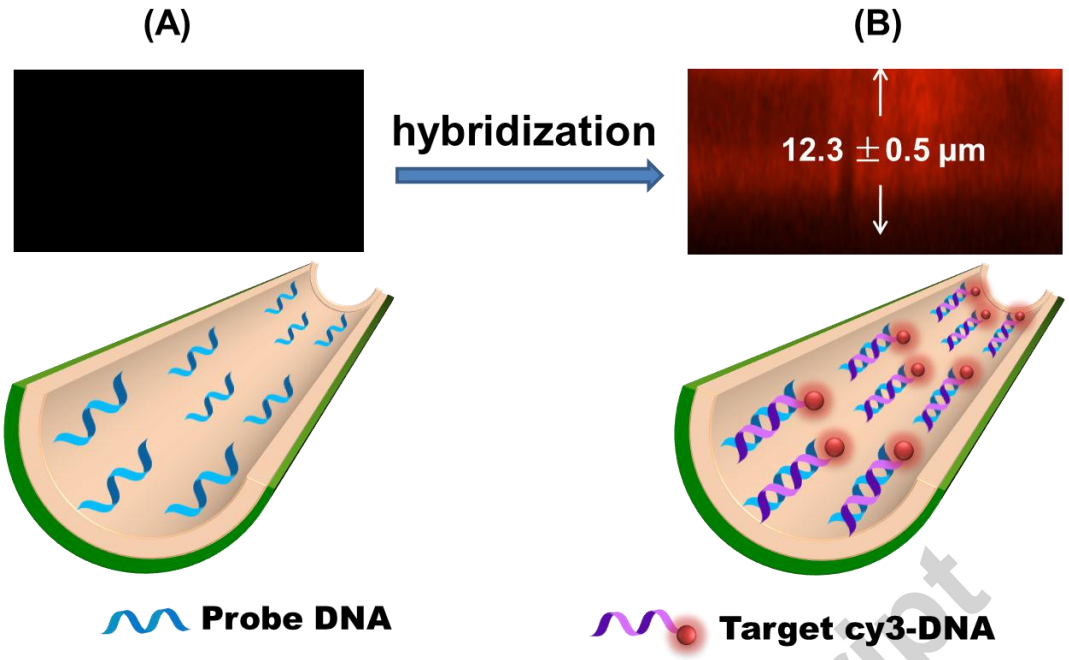

Fig. 3

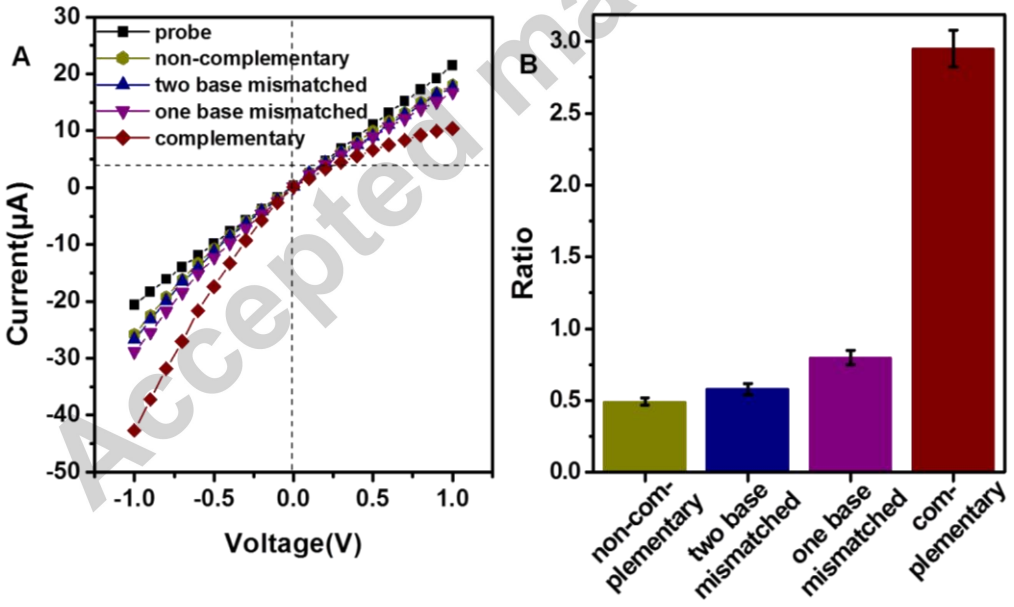

Fig. 4

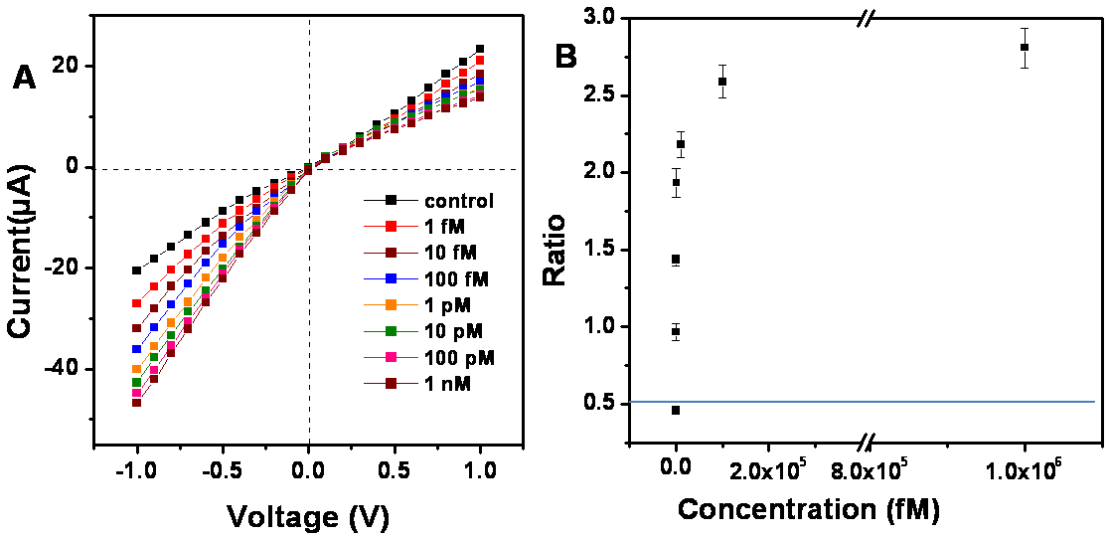

Fig. 5

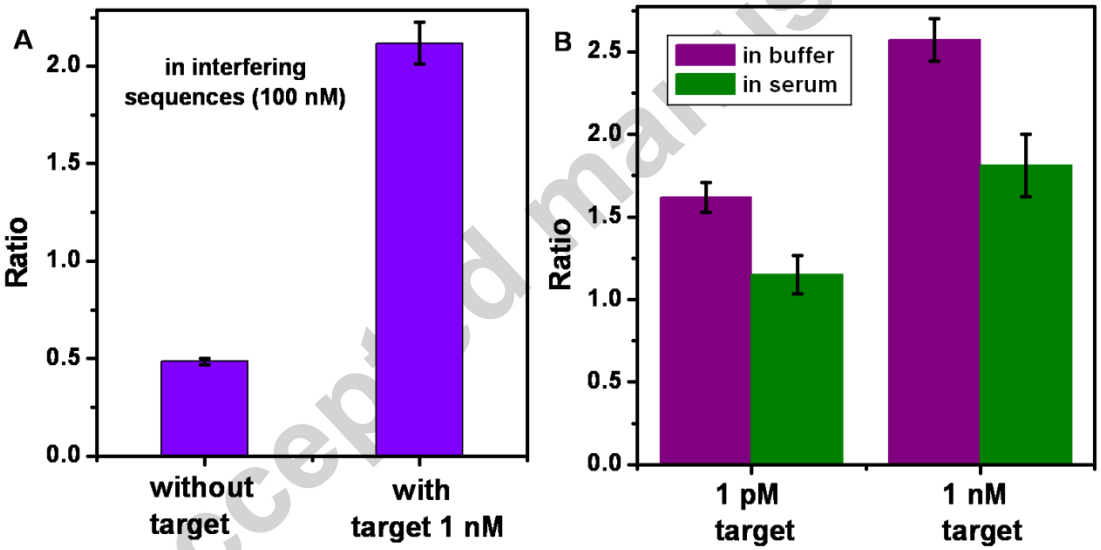

Fig. 6

Highlights

- 3-D nanochannel-based biosensor for DNA detection has been proposed.
- DNA-DNA hybridization has been employed to realize label-free and sensitive detection of DNA by using the fabricated nanochannel biosensor.
- The fabricated nanochannel biosensor is able to detect DNA in interfering system and serum sample.
- High sensitivity has been achieved based on this detection system.
- The developed sensing platform shows good sequence discrimination.